International Journal of Engineering

Journal Homepage: www.ije.ir

RESEARCH NOTE

Hot Corrosion Behavior of Functional Graded Material Thermal Barrier Coating

M. Rahnavard*[a], M. J. Ostad Ahmad Ghorabi[b]

[a] *Mechanical and Industrial Engineering, Islamic Azad University Semnan Branch, Semnan, Iran*
[b] *Faculty of Mechanical and Industrial Engineering, Islamic Azad University Semnan Branch, Semnan, Iran*

PAPER INFO

Paper history:
Received 18 November 2016
Received in revised form 18 December 2016
Accepted 28 December 2016

Keywords:
Thermal Barrier Coating
Functional Grade Material
Plasma Spray
Hot Corrosion
Molten Salt

ABSTRACT

In this paper a functional graded material (FGM) thermal barrier coating (TBC) is prepared using Atmospheric Plasma Spraying (APS) method. The FGM layers were deposited by varying the feeding ratio of CYSZ/NiCrAlY and conventional CYSZ on a NiCrALY-coated Inconel 738 substrates. Hot corrosion behavior, bonding strength and the related failure mechanisms of a conventional TBC and a FGM TBC are investigated. Hot corrosion studies were conducted in presence of 45% Na_2SO_4+ 55% V_2O_5 molten salt at 1000 ^oC temperature. The as-sprayed coatings and heat-treated coatings were characterized by X-ray diffraction (XRD) and scanning electron microscopy (SEM). Exposing to hot corrosion test, the FGM TBC showed better chemical stability and higher life service in comparison to the conventional TBC. As a result, functional graded material thermal barrier coating exhibited very promising potential as a novel TBC material.

***doi**: 10.5829/idosi.ije.2017.30.01a.13*

1. INTRODUCTION

Thermal barrier coatings (TBCs) are used to reduce thermal loss and protect components from high temperatures. These coatings are composite overlays of bond-coating and ceramic coating on a super-alloy substrate [1]. During the past decades, TBCs have been deposited on traditional gas turbines to protect them from thermal degradation and to enhance the operating temperature of the engine [2]. They can be used for different hot metallic parts of gas turbines including transition pieces, combustion lines, first-stage blades and vanes [3].

TBCs are usually applied by an atmospheric Plasma Spray (APS) on substrate surface. Generally, APS method is employed for both top coatings and bond coatings to provide the best joint between them [4]. Plasma sprayed TBCs have a low thermal conductivity accompanied with a good chemical stability at high temperature applications [5]. One of the main concerns of TBCs used in gas turbines is degradation by deposited molten materials resulting from a combination of impurities introduced with the intake air and/or the fuel [6]. Deposition of sodium chlorides onto the turbine blades from air or seawater contamination, combined with the gaseous sulfur oxides during service, can cause hot corrosion attack of TBCs [7].

The most common TBC systems consist of a thermally insulating ceramic topcoat layer over an oxidation resistance bond coat metallic layer. The role of metallic bond coat is to enhance the adherence between the substrate and ceramic topcoat layer [8].

TBC systems have some reliability and durability problems arising from the thermal stresses (induced by thermal expansion mismatch between the ceramic and metal layers) and oxidation. Recently, introduction of an interfacial zone with graded thermomechanical properties between the topcoat layer and bond coat layer, or replacement of coating with composite layer containing varying volume/weight ratio of ceramic/metallic materials are used as the effective ways to overcome the durability problems of conventional TBCs [9]. This type of composite coatings is called functionally graded material (FGM) TBC. It was reported that application of FGM TBCs as coating or interfacial zones between coating layers can reduce the magnitude of residual stresses and increase the

*Corresponding Author's Email: rahnavardmohsen@yahoo.com (M. Rahnavard)

Please cite this article as: M. Rahnavard, M. J. Ostad Ahmad Ghorabi, Hot Corrosion Behavior of Functional Graded Material Thermal Barrier Coating, International Journal of Engineering (IJE), TRANSACTIONS A: Basics Vol. 30, No. 1, (January 2017) 101-108

bonding strength [9, 10]. Different methods of thermal spraying are used for FGM coatings including: (a) Pre-alloyed powders as feedstock in the plasma spraying, (b) powders spraying using two guns, and (c) thermal spraying using a gun with independent powder feed [11].

The aim of this study is the investigation of the hot corrosion resistance behavior of a conventional and a FGM TBCs in presence of molten sulfate and vanadate salt. It is very important to compare the failure mechanism of these two different coatings in order to find potential usage of FGM coating as TBC materials. For this purpose, the failure mechanisms of coatings were investigated by observation of microstructure and chemical analysis before and after hot corrosion test. The influence of microstructure on the properties and performance of coatings are discussed.

2. MATERIALS AND METHODS

2. 1. Materials Inconel 738LC Ni-based super-alloy was employed as substrate material in this study. The substrates were cylindrical specimens of 25mm diameter and 40 mm height. Two kinds of coating materials including conventional Ceria-yttria stabilized zirconia (CYSZ) powders and FGM layer were deposited onto a NiCrAlY bond coat as substrates by commercial APS equipment. The properties of powders are given in Table 1.

2. 2. Methods The surface of the substrate was cleaned with acetone and then sandblasted using silicon carbide before spraying. For conventional TBC, CYSZ top coat was deposited using A-3000 atmospheric plasma spraying equipment (METCO 3MB). For FGM coating, three layers were sprayed by varying the feeding ratio of CYSZ/NiCrAlY powders as shown schematically in Figure 1. The total thickness of both coatings was 500µm, compositions of which are given in Table 2. The spraying parameters of applied coatings are summarized in Table 3.

Hot corrosion study of coatings under presence of sodium sulfate and vanadium oxide mixtures were conducted on samples at 1000 ^{o}C in air. This test was similar to the test conducted by Ahmadi-Pidani et al. [2] and Nejati et al. [12]. For the salt mixture, 45% Na_2SO_4+ 55% V_2O_5 from Merck were used.

The prepared corrosive mixture was uniformly placed onto the surface of TBC specimens with a total

TABLE 1. Physical and chemical specification of powders

Commercial powder	Chemical composition	Particle size (µm)	Morphology
METCO 205NS	ZrO_2 24CeO_2 2.5Y_2O_3	125±11	spherical

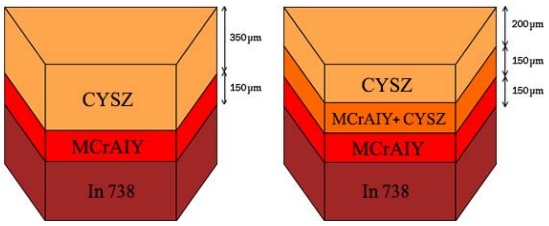

Figure 1. Schematic description of studied plasma coatings, a) Conventional TBC, and b) FGM TBC

TABLE 2. APS spraying parameters for coating

Parameter	Value		
	NiCrAlY	NiCrAlY+CYSZ	CYSZ
Flow rate (A)	450	50	500
Ar/H2 ratio	85/15	85/15	85/15
Powder feeding rate (g/min)	10	15	20
Spray distance (mm)	150	120	80

TABLE 3. Thickness of different coating layers

Layer	Type	
	Conventional TBC	FGM
100% NiCrAlY (µm)	150	150
50% NiCrAliY+ 50% CYSZ (µm)	0	150
100% CYSZ (µm)	350	200
Total thickness (µm)	500	500

weight of 25 mg/cm^2 and 3 mm away from the upper edges, as shown in Figure 2. This distance was employed to avoid failure at the corner or along the edge near the corner. The thermal cycle consisted of 4 h heating up to 1000 ^{o}C and subsequently 1 h cooling down in the oven. The experiments were continued until the occurrence of obvious degradation or debonding of the coatings. Three specimens were used for verification of repeatability of test results.

The microstructure of sprayed and thermally cycled samples were investigated using an optical microscopy and a scanning electron microscope (SEM) equipped with an energy dispersive spectrometer (EDS) for elemental analyses. The crystalline phases of the samples before and after hot-corrosion test were identified by X-ray diffraction on a Unisantis/MD-300 X-ray diffractometer with Cu Ni radiation of 1 mA.

The bonding strength of coatings to the substrate and bond coat was evaluated by a mechanical test according to ASTM C633 [13].

Figure 3 shows the schematic description of the bonding strength test.

Figure 2. Corrosive salt on the coating surface

In this test method, the uncoated specimens were fixed by a screw to the constant fixture of a tensile testing machine. The coated specimen was fixed to the movement fixture in a way that coated surface was attached to uncoated sample using a high performance adhesive. During the test, force and displacement were recorded for specimens and its average was reported.

Microhardness of the layers, including substrate, bond layer (NiCrAlY), composite layer (NiCrAlY+CYSZ) and ceramic top layer (CYSZ) was evaluated before and after hot corrosion test by a MVK-H21 hardness tester from AKASHI Co. with a load of 100 g.

3. RESULTS AND DISCUSSIONS

3. 1. Characterization of As-Sprayed TBCs The SEM cross-section micrograph of the conventional TBC, which is composed of the CYSZ top coat and the NiCrAlY bond coat, is shown in Figure 4a. A sharp interface between the top coating and bond coating layers could be clearly observed. The CYSZ layer has a laminar and porous structure which is the common characteristic of the plasma spraying ceramic coatings [14].

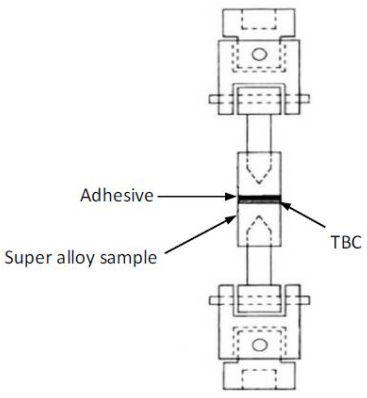

Figure 3. Schematic description of bonding strength test [12]

The higher porosity is also related to the non-molten zirconium oxide during the coating process which results in less plastic deformation of particles upon collision with substrate surface [11]. In comparison to CYSZ layer, NiCrAlY layer has less porosity and uniform structure. The enlarged area of top coat layer for the conventional TBC is shown in Fig. 4b. Two types of porosity, namely voids and micro-cracks were observed on the top coat layer.

Figure 5 represents the x-ray diffraction pattern of the CYSZ top coating. The predominant phase is equilibrium tetragonal zirconia ($t.ZrO_2$) which indicates the perfect deposition. The short peaks in XRD pattern is related to the presence of CeO_2 ($c\text{-}CeO_2$) from stabilizer.

SEM cross-section micrograph of FGM coating is shown in Figure 6. Three different interfaces between layers are determined using SEM micrographs. The first layer is pure NiCrAliY powder directly deposited on the substrate; the second layer is a FGM composite layer (CYSZ+NiCrAlY) in which the top coat layer is pure CYSZ powder. It is hard to distinguish a sharp interface between FGM and top coat layer. The NiCrAlY bond coat layer shows less porous structure due to the fully melted metallic particles. The porous appearance in the FGM layer is due to the presence of non-melted and partially melted CYSZ ceramic powders and lamellar characteristics of thermally sprayed coatings [11]. Due to the use of CYSZ top coating material for both TBCs, the X-ray diffraction pattern of the conventional TBC and the FGM TBC is similar.

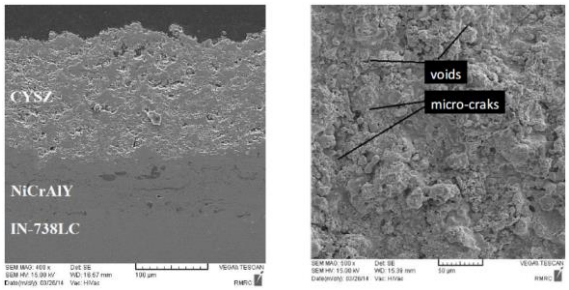

Figure 4. SEM micrographs of: a) cross-sectional of conventional TBC, and b) enlarged picture of top coat layer

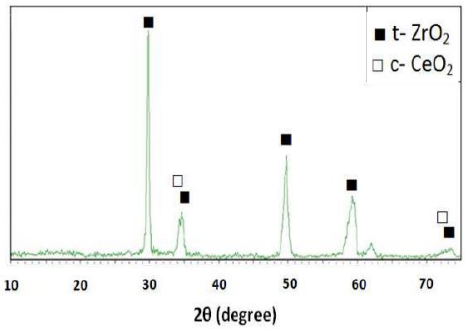

Figure 5. X-ray diffraction pattern of the conventional TBC

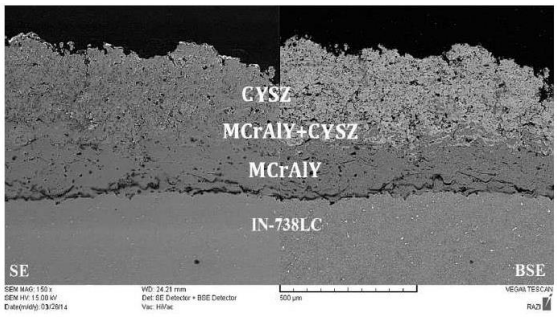

Figure 6. SEM micrographs of the cross-sectional FGM TBC

3. 2. Characterization of TBCs After Hot Corrosion Test The TBCs after hot corrosion test in presence of Na_2SO_4-V_2O_5 salt is shown in Figure 7. The Conventional TBC and the FGM TBC have failed after 24 h and 40 h being exposed to hot corrosion, respectively. Delamination failure could be observed for both TBCs in the metallic bond coat and the ceramic top coat interface. This could be due to possibility of thermally grown oxide (TGO) overgrowth and Zirconia phase transformation near the interface [15]. The thermally grown oxide could be deteriorated in basic or acidic fluxing mechanism. As a result, spallation failure of TBC accompanied by debonding of TGO occurs. The conventional TBC clearly exhibited full delamination and spallation in more area than FGM TBC. The spallation for the FGM TBC occurred only in the edges.

Figure 8 shows the SEM micrographs of the conventional TBC surface after exposure to 24 h hot corrosion test. Comparing the microstructure of the CYSZ top coat before and after hot-corrosion test reveals the laminar and continuous structure (Figure 4) is transformed to a porous structure due to the hot-corrosion operation (Figure 8a). This could be attributed to the zirconia transformation during the process. Three different phases were clearly observed on the top surface which is indicated as A, B and C in enlarged images (Figure 8b). The EDS analysis of the materials which is marked by points A, B and C in Fig. 8b, is presented in Figure 9.

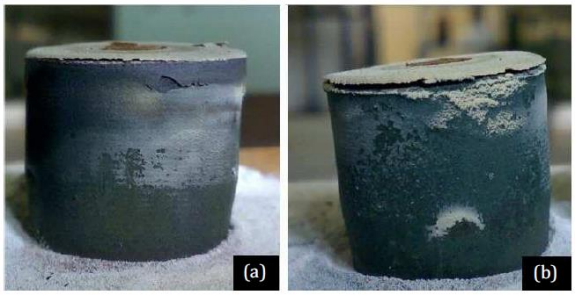

Figure 7. Specimens after hot-corrosion test at 1000 ◦C: a) FGM TBC for 40 h, and b) TBC for 24 h

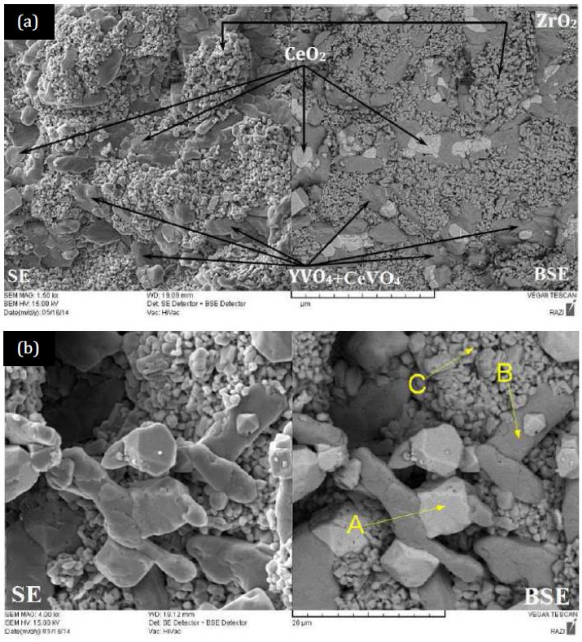

Figure 8. SEM micrograph of: a) the top surface of the conventional TBC after 24 h exposure to the hot-corrosion test, b) enlarged picture

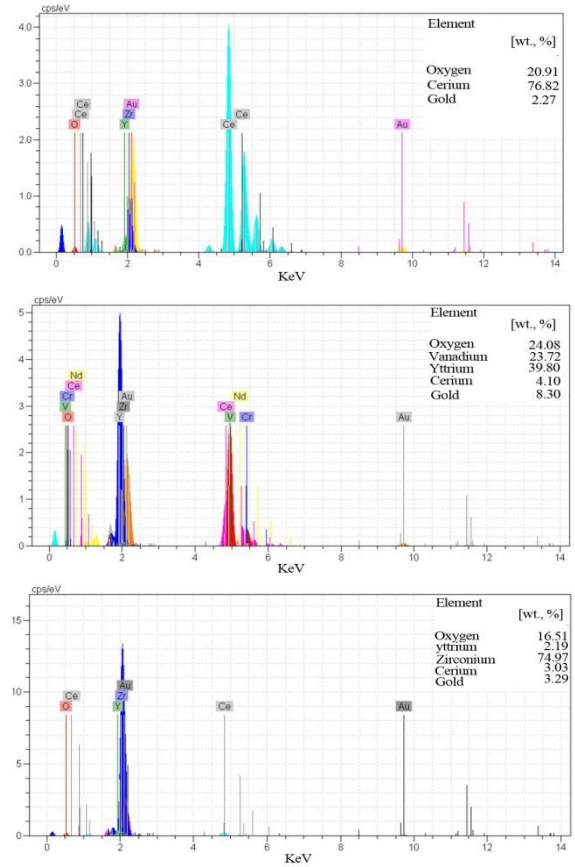

Figure 9. EDX analysis of points on Figure 8b : (a) A, (b) B, and (c) C

It revealed that the white crystals "A" contained Ce, and O, the gray rod-type crystals "B" had Y, V, O and little Ce, and the fine crystals "C" had Zr and O elements. According to the results of EDS analysis, crystals in "A", "B" and "C" refer to CeO_2, $CeVO_4$+YVO_4, and substrate zirconia (CYSZ), respectively.

SEM micrograph of the top surface of the FGM TBC is presented in Fig. 10a. Similar to the conventional TBC, three different phases are distinguished in the surface of the coating. The observed crystals are marked with "A", "B" and "C" in enlarged SEM image as shown in Figure 10b. EDX analysis on this points revealed that the white crystals "A", gray crystals "B" and crystals "C" are attributed to the CeO_2, blended YVO_4+$CeVO_4$ crystals and zirconia, respectively.

$CeVO_4$ and YVO_4 crystals are the main products and the CeO_2 is the by-product of the hot-corrosion process. Besides, generation and rapid growing of the products of hot-corrosion process is as an indication for progress in hot-corrosion process [12]. Therefore, comparing the amount and size of products during this process could be used for evaluation of the progress in hot-corrosion cycles.

Identified YVO_4+$CeVO_4$ crystals in the conventional TBC are longer and thicker in comparison to the FGM TBC. It could be concluded that despite of the greater exposure time to the hot-corrosion process accompanied with generation of fine and less corrosive products, FGM TBC have better resistance.

Generation of smaller and lesser corrosive products for the FGM TBC after exposure to hot-corrosion indicates that low amount of CYSZ were removed from the structure and reacted with corrosive salt. Therefore, little transformation of zirconia occurred which resulted in smaller increment of volume and longer stability of coating against hot-corrosion cycles. Transformation of tetragonal zirconia to monoclinic zirconia is accompanied with increase in volume by 3-5%. This could be due to the presence of active elements for reaction with corrosive salt in the NiCrAlY+CYSZ graded layer. Indeed, penetrated O_2 and V_2 molecules into the coating are consumed for the reaction with active metallic elements including Al and Cr, so there is a limited possibility for the reaction with zirconia (yttrium and cerium). Hence, occurrence of coating degradation due to the transformation of tetra zirconia to monoclinic zirconia is limited.

SEM micrographs and EDS elemental mapping for Al, Cr, Zr, Y and V at the cross-section of the coating after hot-corrosion cycles for the conventional TBC and the FGM TBC are shown in Figure 11 and Figure 12, respectively. Elemental distribution in depth of the coating and under-coating after hot-corrosion test are shown in these figures.

Figure 11 shows that the thickness of the coating is less than 500µm. According to the elemental mapping it was indicated that Cr and Al remained on the top surface which were the main elements for NiCrAlY layer.

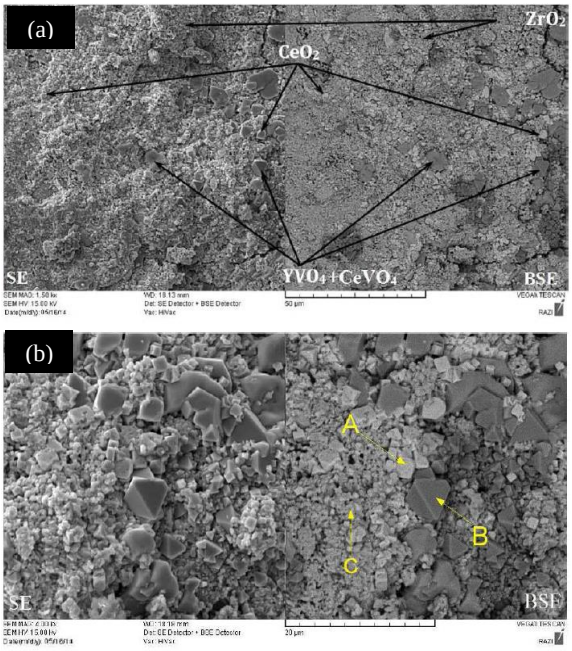

Figure 10. SEM micrograph of: a) the top surface of FGM TBC after 40 h exposure to hot-corrosion test, and b) enlarged picture

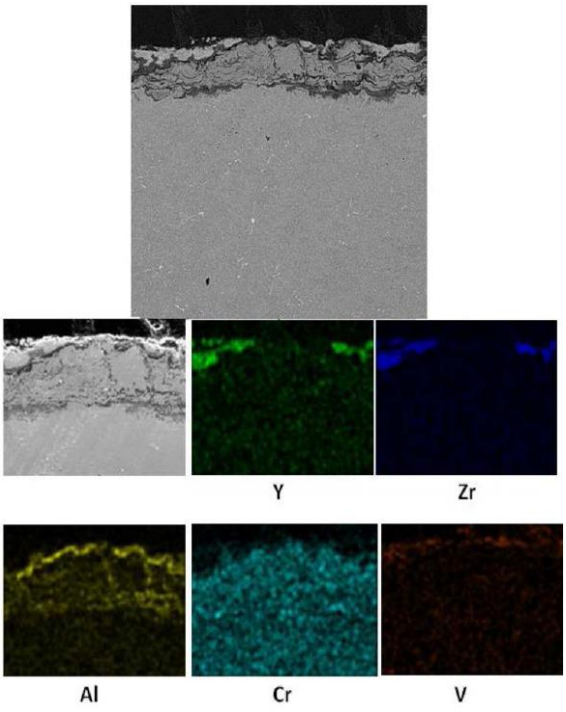

Figure 11. SEM micrographs and EDX elemental mapping of the conventional TBC after hot-corrosion test

Also, low concentration of yttria, vanadium and zirconia are observed in the top boundary of the top coatings. It could be concluded that the coating was separated due to the growth of TGO layer at the bond coat layer/topcoat layer interface. On the basis of previous findings, one of the degradation mechanisms of bond coat is due to the infiltration of salts and oxygen [16, 17]. As can be seen, in addition to corrosion degradation, chemical reactions were responsible for the degradation of bond coat.

SEM micrographs of FGM TBC (Figure 12) show that the debonded region is an interlaminar NiCrAlY+CYSZ composite layer. Presence of microcracks in the vertical direction of the interface between bond coat and the substrate indicates that corrosion occurred in the bond coat layer. It should be noted that the main mechanism for the degradation of composite layer is due to the removal of zirconia from yttria and cerum. This mechanism results in the phase transformation and increasing the volume of material.

3. 3. XRD Analysis X-ray diffraction patterns of the conventional TBC and the FGM TBC after exposure to 1000 ^{o}C hot-corrosion cycles are shown in Figure 13. In addition to the presence of tetragonal ZrO_2, monoclinic ZrO_2, YVO_4+$CeVO_4$ and CeO_2 crystals are generated on the TBC surface. In spite of the similar crystals to the conventional TBC, the presence of $AlVO_4$ and $CrVO_4$ on the surface of FGM TBC is evident. X-ray pattern of the FGM TBC indicates that identified YVO_4 and $CeVO_4$ are decreased in this sample. On the basis of the results, monoclinic ZrO_2, YVO_4+$CeVO_4$, CeO_2, $CrVO_4$ and $AlVO_4$ could be introduced as the products of hot-corrosion process in 1000 ^{o}C [18].

SEM and XRD analysis of the FGM TBC revealed smaller size of YVO_4+$CeVO_4$ crystals and lower intensity in X-ray pattern in comparison to the conventional TBC. These results confirmed that the FGM TBC is more corrosion resistant than the conventional TBC. XRD patterns of the coating surface after hot-corrosion cycles indicated lower transformation of zirconia for the FGM TBC in comparison to the conventional TBC.

3. 4. Hardness of the Coatings The hardness value of all coating layers before and after hot-corrosion test are measured and given in Table 4. According to the results, hardness of the layers increased after exposure to hot-corrosion test. Increase in the hardness of the coatings should be attributed to the formation of hard oxide products.

Formation of oxide crystals such as CeO_2, YVO_4 and $CeVO_4$ is the main reason for the increment in hardness of the coating. The size of these crystals is greater than microhardness probe and they have relatively high distribution in coating surface. Therefore, possibility of impact between probe and these hard crystals is very high. Furthermore, formation of monoclinic zirconia as a hot-corrosion product induced a compression stress to the coating that causes coating hardening, while tensile stress causes reduction in hardening of the coating [19].

In general, infiltration of oxygen into the bond coat layer caused formation of oxide products which is the primary reason for the increase in coating hardness after the hot corrosion test. For the FGM TBC, in addition to the penetration of oxygen into the composite layer, the formation of metal oxides (i.e. ZnO_2 and Al_2O_3) and ceramic oxides (i.e. CeO_2, $CeVO_4$ and YVO_4) are responsible for the increase in the coating hardness.

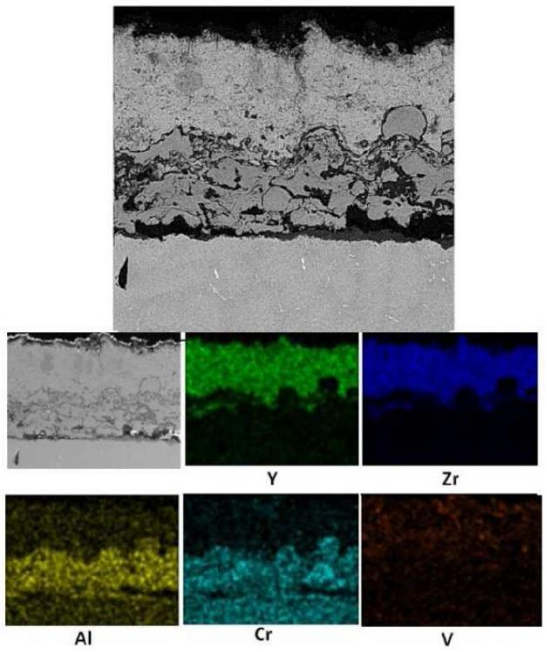

Figure 12. SEM micrographs and EDS elemental mapping of the FGM TBC after hot-corrosion test

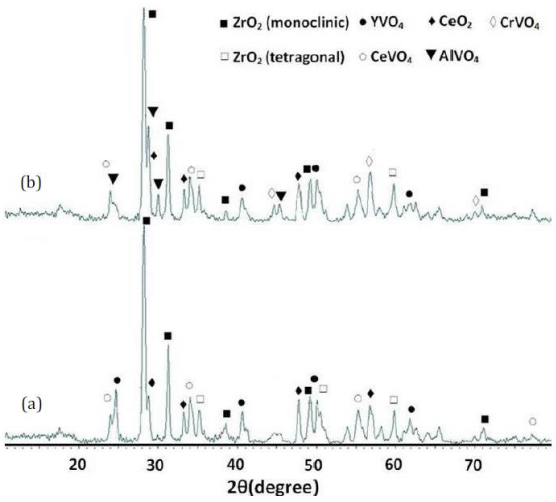

Figure 13. XRD patterns of the coating after hot-corrosion in 1000 ˚C: a) Conventional TBC, and b) FGM TBC

TABLE 4. Hardness of coating layers before and after hot corrosion test

Layer		Type	
		Before hot corrosion	After hot corrosion
Conventional TBC	Inconel	450	435
	NiCrAlY	515	561
	CYSZ	623	683
FGM TBC	Inconel	428	443
	NiCrAlY	508	526
	NiCrAlY+CYSZ	570	595
	CYSZ	597	664

3. 5. Bonding Strength Bonding strength of the conventional TBC and the FGM TBC was measured and shown in Figure 14. The bonding strength of the FGM TBC was 54% greater than the conventional TBC. This is the reason of the gradually change from ceramic to metallic nature in the composite layer, which reduced thermal stresses at CYSZ/NiCrAlY interface and eliminated internal tensile stresses [20].

For the conventional TBC, fracture occurred at the CYSZ/NiCrAlY interface which can be seen in figure 15a. As shown in Fig. 15b, in the case of FGM TBC, fracture occurred in the composite layer (CYSZ+NICrAlY).

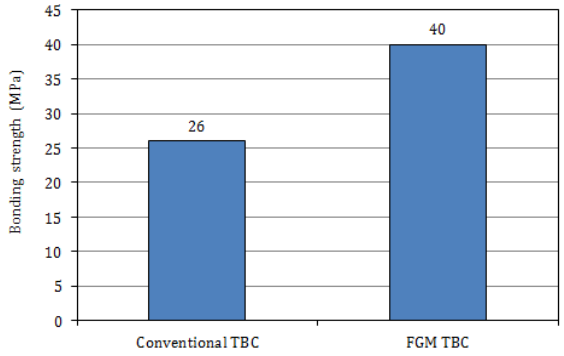

Figure 14. Comparison of bonding strength of coatings

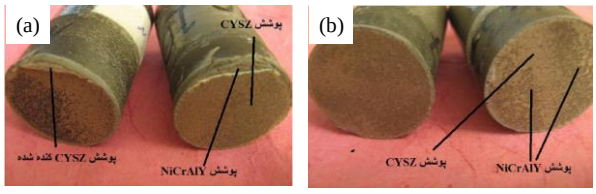

Figure 15. Fracture of coatings after cohesive strength, a) Conventional TBC, and b) FGM-TBC

4. CONCLUSION

In this study, CYSZ+NiCrAlY composite layer was successfully deposited on a superalloy substrate as FGM layer. Hot corrosion and mechanical behavior of the prepared FGM TBC and a conventional TBC was evaluated. Based on the obtained results, the following conclusions can be drawn:

- The results indicated that the hot-corrosion resistance of super-alloy materials can be improved marginally by employing FGM coating. The life service of the FGM TBC was greater than the conventional TBC. The Conventional TBC and the FGM TBC were degraded after exposure to 24h and 40h hot-corrosion cycles, respectively.
- The conventional TBC exhibited full delamination and spallation in more area than the FGM TBC. The spallation for the FGM TBC was occurred only in the edges.
- It can be concluded that the FGM coating failed due to the growth of thermally grown oxide (TGO) layer at the bond coat layer/topcoat layer interface.
- The hardness of both coatings after the hot-corrosion test was increased. It was believed that the formation of oxide crystals such as CeO_2, YVO_4 and $CeVO_4$ are responsible for increment in coating hardness.

Bonding strength of the FGM TBC was 54% greater than the conventional TBC. It was mainly due to the improvement of fracture toughness of the FGM layer.

5. REFERENCES

1. Goswami, B., Ray, A.K. and Sahay, S., "Thermal barrier coating system for gas turbine application-a review", ***High Temperature Materials and Processes***, Vol. 23, No. 2, (2004), 73-92.
2. Ahmadi-Pidani, R., Shoja-Razavi, R., Mozafarinia, R. and Jamali, H., "Evaluation of hot corrosion behavior of plasma sprayed ceria and yttria stabilized zirconia thermal barrier coatings in the presence of $Na_2SO_4^+$ V_2O_5 molten salt", ***Ceramics International***, Vol. 38, No. 8, (2012), 6613-6620.
3. Cao, X., Vassen, R. and Stoever, D., "Ceramic materials for thermal barrier coatings", ***Journal of the European Ceramic Society***, Vol. 24, No. 1, (2004), 1-10.
4. Moskal, G., "Thermal barrier coatings: Part 1–characteristics of microstructure and properties, generation and directions of development of bond", ***Archives of Materials Science***, Vol. 28, No. 1-4, (2007), 100-112.
5. Ma, X., Cho, S. and Takemoto, M., "Acoustic emission source analysis of plasma sprayed thermal barrier coatings during four-point bend tests", ***Surface and Coatings Technology***, Vol. 139, No. 1, (2001), 55-62.
6. Levi, C.G., Hutchinson, J.W., Vidal-Setif, M.-H. and Johnson, C.A., "Environmental degradation of thermal-barrier coatings by molten deposits", ***MRS Bulletin***, Vol. 37, No. 10, (2012), 932-941.

7. Xiaoyun, X., Hongbo, G., Shengkai, G. and Huibin, X., "Hot corrosion behavior of double-ceramic-layer lati 2 al 9 o 19/ysz thermal barrier coatings", ***Chinese Journal of Aeronautics***, Vol. 25, No. 1, (2012), 137-142.
8. Rahimipour, M. and Mahdipoor, M., "Comparative study of plasma sprayed yittria and ceria stabilized zirconia properties", ***International Journal of Engineering-Transactions A: Basics***, Vol. 26, No. 1, (2012), 13.
9. Yildirim, B. and Erdogan, F., "Edge crack problems in homogenous and functionally graded material thermal barrier coatings under uniform thermal loading", ***Journal of Thermal Stresses***, Vol. 27, No. 4, (2004), 311-329.
10. Lee, Y. and Erdogan, F., "Residual/thermal stresses in fgm and laminated thermal barrier coatings", ***International Journal of Fracture***, Vol. 69, No. 2, (1994), 145-165.
11. Saeedi, B., Sabour, A. and Khoddami, A., "Study of microstructure and thermal shock behavior of two types of thermal barrier coatings", ***Materials and Corrosion***, Vol. 60, No. 9, (2009), 695-703.
12. Nejati, M., Rahimipour, M. and Mobasherpour, I., "Evaluation of hot corrosion behavior of CSZ, CSZ/micro Al_2O_3 and csz/nano Al_2O_3 plasma sprayed thermal barrier coatings", ***Ceramics International***, Vol. 40, No. 3, (2014), 4579-4590.
13. C633, A., " Adhesion or cohesion strength of thermal spray coatings".
14. Loghman-Estarki, M.R., Nejati, M., Edris, H., Razavi, R.S., Jamali, H. and Pakseresht, A.H., "Evaluation of hot corrosion behavior of plasma sprayed scandia and yttria co-stabilized nanostructured thermal barrier coatings in the presence of molten sulfate and vanadate salt", ***Journal of the European Ceramic Society***, Vol. 35, No. 2, (2015), 693-702.
15. Song, Y., Zhou, C. and Xu, H., "Corrosion behavior of thermal barrier coatings exposed to nacl plus water vapor at 1050°c", ***Thin Solid Films***, Vol. 516, No. 16, (2008), 5686-5689.
16. Wellman, R. and Nicholls, J., "Erosion, corrosion and erosion–corrosion of EB PVD thermal barrier coatings", ***Tribology International***, Vol. 41, No. 7, (2008), 657-662.
17. Kramer, S., Yang, J., Levi, C.G. and Johnson, C.A., "Thermochemical interaction of thermal barrier coatings with molten CaO–MgO– Al_2O_3–SiO_2 (cmas) deposits", ***Journal of the American Ceramic Society***, Vol. 89, No. 10, (2006), 3167-3175.
18. Mohan, P., Patterson, T., Desai, V. and Sohn, Y., "Degradation of free-standing air plasma sprayed conicraly coatings by vanadium and phosphorus pentoxides", ***Surface and Coatings Technology***, Vol. 203, No. 5, (2008), 427-431.
19. Afrasiabi, A. and Kobayashi, A., "Hot corrosion control in plasma sprayed ysz coating by alumina layer with evaluation of microstrcuture and nanoindentation data (H,E)", ***Vacuum***, Vol. 88, No., (2013), 103-107.
20. Khoddami, A., Sabour, A. and Hadavi, S., "Microstructure formation in thermally-sprayed duplex and functionally graded nicraly/yttria-stabilized zirconia coatings", ***Surface and Coatings Technology***, Vol. 201, No. 12, (2007), 6019-6024.

Hot Corrosion Behavior of Functional Graded Material Thermal Barrier Coating

RESEARCH NOTE

M. Rahnavard[a], M. J. Ostad Ahmad Ghorabi[b]

[a] *Mechanical and Industrial Engineering, Islamic Azad University Semnan Branch, Semnan, Iran*
[b] *Faculty of Mechanical and Industrial Engineering, Islamic Azad University Semnan Branch, Semnan, Iran*

P A P E R I N F O

Paper history:
Received 18 November 2016
Received in revised form 18 December 2016
Accepted 28 December 2016

Keywords:
Thermal Barrier Coating
Functional Grade Material
Plasma Spray
Hot Corrosion
Molten Salt

چکیده

در این مطالعه، یک پوشش سد حرارتی چندلایه (FGM) توسط روش پاشش پلاسما با هوا تولید شده است. لایه‌های سد حرارتی FGM با درصدهای مختلف تغذیه CYSZ/NiCrAlY و لایه سد حرارتی معمولی CYSZ بر روی یک زمینه اینکونل ۷۳۸ پوشش داده شدند. سپس، رفتار خوردگی داغ، مقاومت چسبندگی و مکانیزم‌های تخریب مربوطه برای یک پوشش سد حرارتی معمولی و چندلایه FGM بررسی شد. مطالعه خوردگی داغ در حضور نمک مذاب ٪۴۵ Na_2SO_4 + ٪۵۵ V_2O_5 در دمای ۱۰۰۰ درجه سانتی‌گراد انجام شده است. پوشش‌های قرار گرفته در معرض حرارت به وسیله آنالیزهای XRD و SEM تحلیل شدند. بررسی نتایج نشان داد که پوشش سد حرارتی چندلایه FGM نسبت به پوشش سد حرارتی معمولی دارای پایداری شیمیایی و عمر سرویس دهی بیشتری در هنگام مواجهه با خوردگی داغ می‌باشد. همچنین، پوشش‌های سد حرارتی چندلایه FGM توانسته‌اند پتانسیل زیادی را از خود جهت مواد پوششی جدید بروز دهند.

***doi**: 10.5829/idosi.ije.2017.30.01a.13*